Hindawi
Journal of Nanomaterials
Volume 2018, Article ID 7545914, 6 pages
https://doi.org/10.1155/2018/7545914

Research Article

Hole Transport Behaviour of Various Polymers and Their Application to Perovskite-Sensitized Solid-State Solar Cells

Jeongmin Lim, Seong Young Kong, and Yong Ju Yun

Department of Energy Engineering, Konkuk University, Seoul 05029, Republic of Korea

Correspondence should be addressed to Yong Ju Yun; yjyun@konkuk.ac.kr

Received 1 February 2018; Revised 15 May 2018; Accepted 29 May 2018; Published 25 June 2018

Academic Editor: Iftikhar Ali Sahito

Inorganic-organic mesoscopic solar cells become a promising alternative for conventional solar cells. We describe a $CH_3NH_3PbI_3$ perovskite-sensitized solid-state solar cells with the use of different polymer hole transport materials such as 2,2′,7,7′-tetrakis-(N,N-di-p-methoxyphenyl-amine)-9,9′-spirobifluorene (spiro-OMeTAD), poly(3-hexylthiophene-2,5-diyl) (P3HT), and poly[[4,8-bis[(2-ethylhexyl)oxy]benzo[1,2-b:4,5-b′]dithiophene-2,6-diyl][3-fluoro-2-[(2-ethylhexyl)carbonyl]thieno[3,4-b]thiophenediyl]] (PTB7). The device with a spiro-OMeTAD-based hole transport layer showed the highest efficiency of 6.9%. Interestingly, the PTB7 polymer, which is considered an electron donor material, showed dominant hole transport behaviors in the perovskite solar cell. A 200 nm thin layer of PTB7 showed comparatively good efficiency (5.5%) value to the conventional spiro-OMeTAD-based device.

1. Introduction

The third-generation photovoltaic devices such as thin-film solar cells, organic solar cells, and solid-state solar cells are considered to be a promising energy conversion devices due to their ease of fabrication and cost-effective materials. Although highly efficient solar cells have already been commercialized based on silicon and other semiconductor materials, the fabrication cost of those photovoltaic devices is still expensive that prevents the technology from reaching widespread consumers. Generally, the purification of silicon-based materials involves high-temperature processing, and the device fabrication of such highly efficient solar cells relies on the vacuum deposition or/and thermal treatment methods which potentially increase the manufacturing cost and decrease the productivity. Third-generation solar cells such as dye-sensitized solar cells [1–5], quantum dot solar cells [6–9], and organic solar cells [10–13] are developed with various structures and diverse material applications. However, the theoretical maximum efficiency performances were far above with those of solar cells due to the energy losses or low dielectric [14]. Recently, a new class of light-absorbing material based on perovskite-structured organolead trihalide ($CH_3NH_3PbI_3$) compound has been synthesized for the development of high-efficiency solid-state solar cells [15]. A device using a thin layer of organolead trihalide perovskite as the light absorber and thin TiO_2- or Al_2O_3-based nanoporous scaffold layers could be fabricated using a simple solution process [15–17]. The active research on perovskite solar cell is blooming nowadays. For example, the role of mixed halide ($CH_3NH_3PbI_3$-xCl_x) perovskite with alumina scaffold layer enhances a faster electron transport [17]; Eperon et al. have reported on the PCE of 11.4% using the morphology-controlled perovskite photoactive layer [18]; Carnie et al. simplified a fabrication process of photoactive layer and achieved a power conversion efficiency (PCE) of 7.16% [19]; Heo et al. reported a PCE of 12% by replacing the spiro-OMeTAD hole transport materials with polytriarylamine (PTAA) polymer [20]; and other researchers represent a two-step deposition of perovskite materials for uniformly coated layer [21, 22]. One of the essential qualifications for the high efficiency of solar cells is a proper balance of series and shunt resistance. However, because of the high conductivity of perovskite materials, it demands a thick layer of HTM to evade the imbalance or pinhole effect [23, 24]. Due to these drawbacks, a thick layer of HTM was necessary, even though they have less conductivity with high series resistance. Herein, we investigated the roles of different

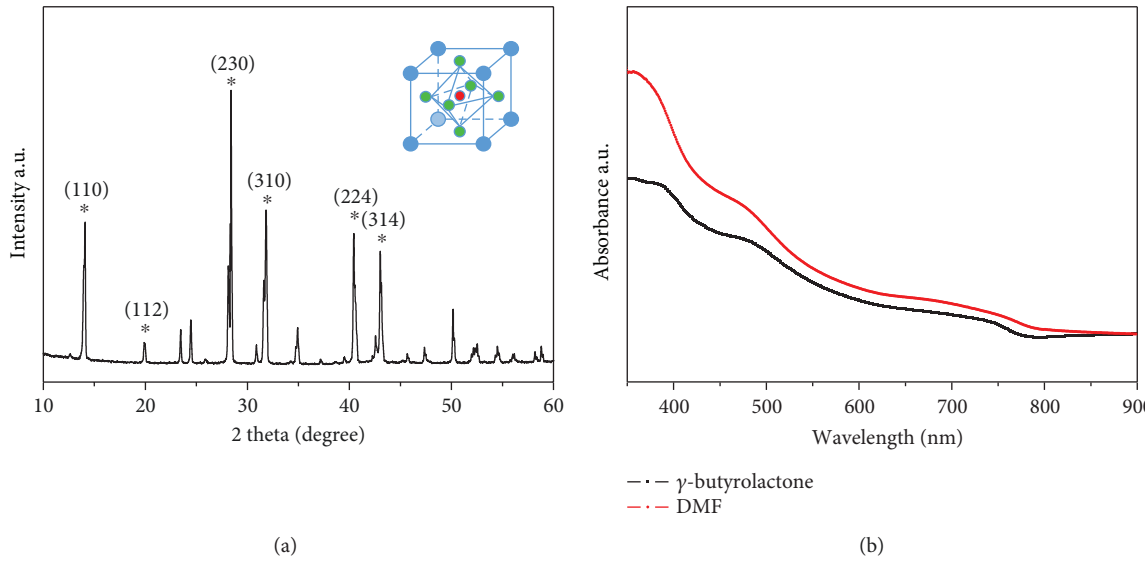

FIGURE 1: (a) X-ray diffraction of $CH_3NH_3PbI_3$ perovskite materials prepared as powder form and inset shows tetragonal structure of materials. (b) UV-visible spectra prepared from γ-butyrolactone (GBL) and dimethylformamide (DMF). $*$ indicates the XRD peaks of CH3NH3PbI3 perovskite materials.

HTMs on the performance of solid-state perovskite solar cells. The fluorine-doped tin oxide (FTO) glass was used as the substrate; a synthesized $CH_3NH_3PbI_3$ perovskite as a light absorber (electron donor); the polymers such as 2,2′,7,7′-tetrakis-(N,N-di-p-methoxyphenyl-amine)-9,9′-spirobifluorene (spiro-OMeTAD), poly(3-hexylthiophene-2,5-diyl) (P3HT), and poly[[4,8-bis[(2-ethylhexyl)oxy]-benzo[1,2-b:4,5-b′]dithiophene-2,6-diyl][3-fluoro-2-[(2-ethylhexyl)carbonyl]thieno[3,4-b]thiophenediyl]] (PTB7) as hole transport materials; and a sputtered gold grid as the counter electrode.

2. Materials and Methods

2.1. Perovskite Materials. The methylammonium perovskite material ($CH_3NH_3PbI_3$) was synthesized according to the previously reported method [15]. A hydroiodic acid (30 mL, 57 wt.% in water, Aldrich) was mixed with methylamine (27.8 mL, 0.273 mol, 40% in methanol; TCI) at 0°C in ice bath with continuous stirring for 2 h. After stirring, the resulting solution was evaporated in a vacuum oven, and the methyl ammonium iodide (CH_3NH_3I) compound was formed. The synthesized product was washed with diethyl ether for three times and then dried under vacuum without further purification; a formation of white coloured powder is an indication of purified methyl ammonium iodide precursor. To prepare the final product of $(CH_3NH_3)PbI_3$, the 1 : 1 molar ratio of methylammonium iodide and lead (II) iodide was dissolved in anhydrous γ-butyrolactone (GBL) and then continuously stirred at 60°C temperature overnight.

2.2. Solar Cell Fabrication. Fluorine-doped tin oxide (FTO) glasses (Pilkington, TEC-8, 8 Ω/sq) were washed with a detergent solution and then cleaned in an ultrasonic bath for 5 min using an ethanol–acetone solution ($v/v = 1/1$) and 2-propanol, in turn, and then further cleaned with the oxygen plasma treatment for the duration of 15 min. A 600 Å thin layer of dense TiO_2 blocking layer was deposited on the FTO glass using the RF sputtering method. A commercial TiO_2 paste (CCIC 18NT) diluted with terpineol was used as a precursor, and the mesoporous TiO_2 layer was deposited on the blocking layer using the spin-coating (4500 rpm, 40 sec) technique. The coated layer was annealed in air atmosphere at 500°C for 1 h and then cooled to room temperature. The perovskite liquid is subsequently coating on the TiO_2 layer using spin coater at 2500 rpm for 40 seconds followed by annealing at 100°C for 20 min. For the deposition of the hole transport layer, different hole transport materials (HTM) are coated onto a perovskite film using the spin coater with a speed of 2500 rpm for 40 sec. To fabricate the counter electrode, 70 nm Au electrode was deposited onto the hole transport layer using the thermal evaporation method.

2.3. Composition of HTM. The spiro-OMeTAD-based HTM was prepared by mixing 170 mM concentration of 2,2′,7,7′-tetrakis-(N,N-di-p-methoxyphenyl-amine)-9,9′-spirobifluorene (spiro-OMeTAD, Merk), 198 mM concentration of 4-tert-butylpyridine (TBP, 96%, Aldrich), and 64 mM concentration of bis(trifluoromethane) sulfonimide lithium salt (LiTFSI, 99.95%, Aldrich) together using a cocktail solvent of chlorobenzene and acetonitrile ($1/0.1 = v/v$). The P3HT-based HTM solution was prepared by dissolving P3HT (Aldrich) in a chlorobenzene solvent with the concentration of 13 mg/mL. Likewise, PTB7 was also dissolved in chlorobenzene with the concentration of 12 mg/mL.

2.4. Characterization. The active area of the cell was measured by an optical microscope (Olympus), and the thickness of the mesoporous TiO_2 layer was analysed by a surface profilometer (P-6, KLA-Tencor). The photovoltaic properties of the cells were measured using a Keithley

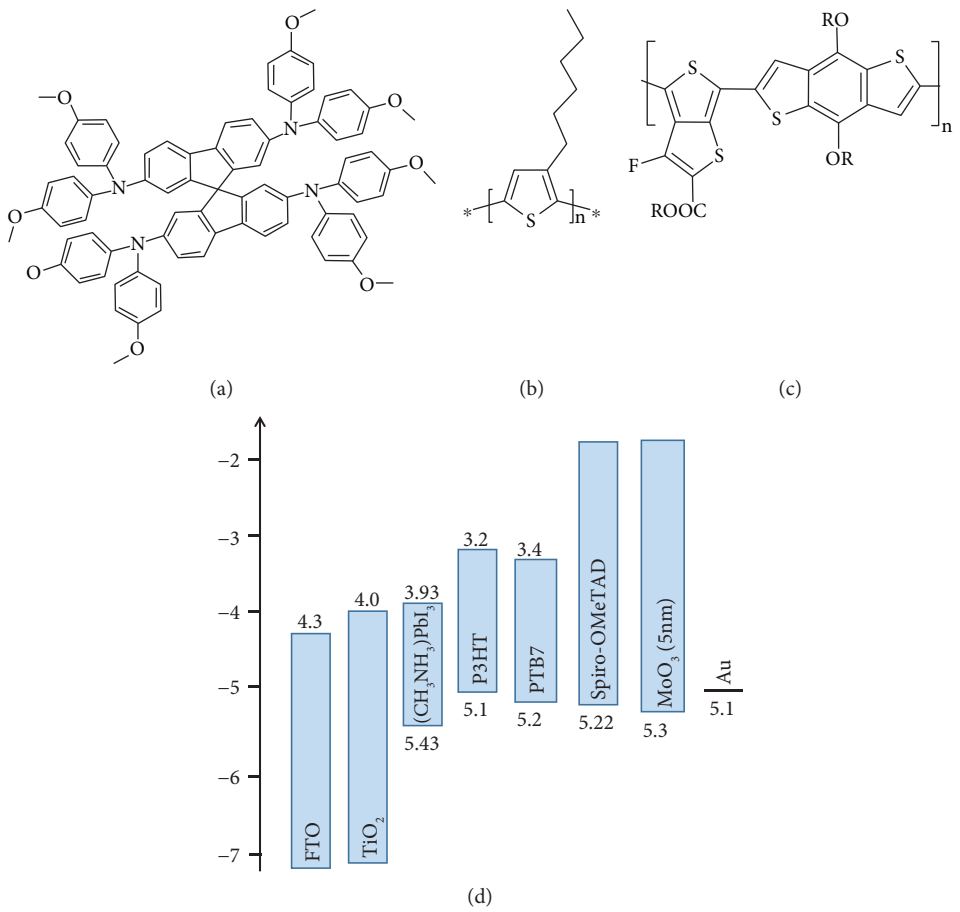

Figure 2: Molecular structure of hole conductor materials of (a) spiro-OMeTAD, (b) P3HT, and (c) PTB7. (d) Energy diagram of materials which was used in this study.

Table 1: The levels of HOMO, LUMO, and hole mobility of THM materials.

	HOMO	LUMO	Hole mobility
Spiro-OMeTAD			$\sim 10^{-5}$ cm^2/V·sec
P3HT	−5.1	−3.2	$\sim 10^{-1}$ cm^2/V·sec
PTB7	−5.15	−3.31	$\sim 10^{-3}$ cm^2/V·sec

2400 digital source meter under the irradiation of a solar simulator (AM 1.5 G, 100 mW/cm2, Sol3A, class AAA, Oriel) as a light source. Irradiation of 1 sun was calibrated by using a certified standard reference cell (PV Measurement Inc.). The photovoltaic performance has been characterized by the measurement of Voc, Jsc, fill factor, and overall efficiency values obtained from the J-V curve. The incident photon to current conversion efficiency (IPCE) spectra was measured using a PV measurement (PV Measurement Inc., QEX7 series), and cross-sectional morphology of the solid state solar cell was analysed by a field-emission scanning electron microscopy (FE-SEM, Nano230, FEI Co.).

3. Result and Discussion

Here, we fabricated a new bilayer heterojunction with organic-inorganic materials onto the nanoporous or mesoporous TiO_2 film. The surface-decorated metal-halide perovskite materials with the formula of ($C_nH_{2n+1}NH_3$) MX (M = Pb;X = I, Br, Cl) were infiltrated within a TiO_2 matrix, which has a key function of light absorption process. The various organic materials have p-type hole transport properties and are thus referred to as HTMs.

Figure 1(a) shows the powder X-ray diffraction (XRD) peaks of the crystalline perovskite materials. There are six sharp reflection peaks such as (110), (112), (220), (310), (224), and (314) that were observed which confirm the tetragonal perovskite structure (include here any JCPDS number available). The inset of Figure 1(a) shows a tetragonal crystal structure of ($C_nH_{2n+1}NH_3$) MX perovskite material. The perovskite material was dissolved into γ-butyrolactone (GBL) or dimethylformamide (DMF) and then coated on the glass plate using spin-coating method. The UV-vis spectrum of the thin perovskite material is measured for the range of 350–900 nm wavelength. From the UV-vis spectra, the synthesized perovskite material absorbs wide range of solar spectrum from the visible to near-infrared region as shown in Figure 1(b). To maximize the energy harvested by the solar cells, light-absorbing materials with wide spectral response ranges could expand the absorbance throughout the visible spectrum. From the observed

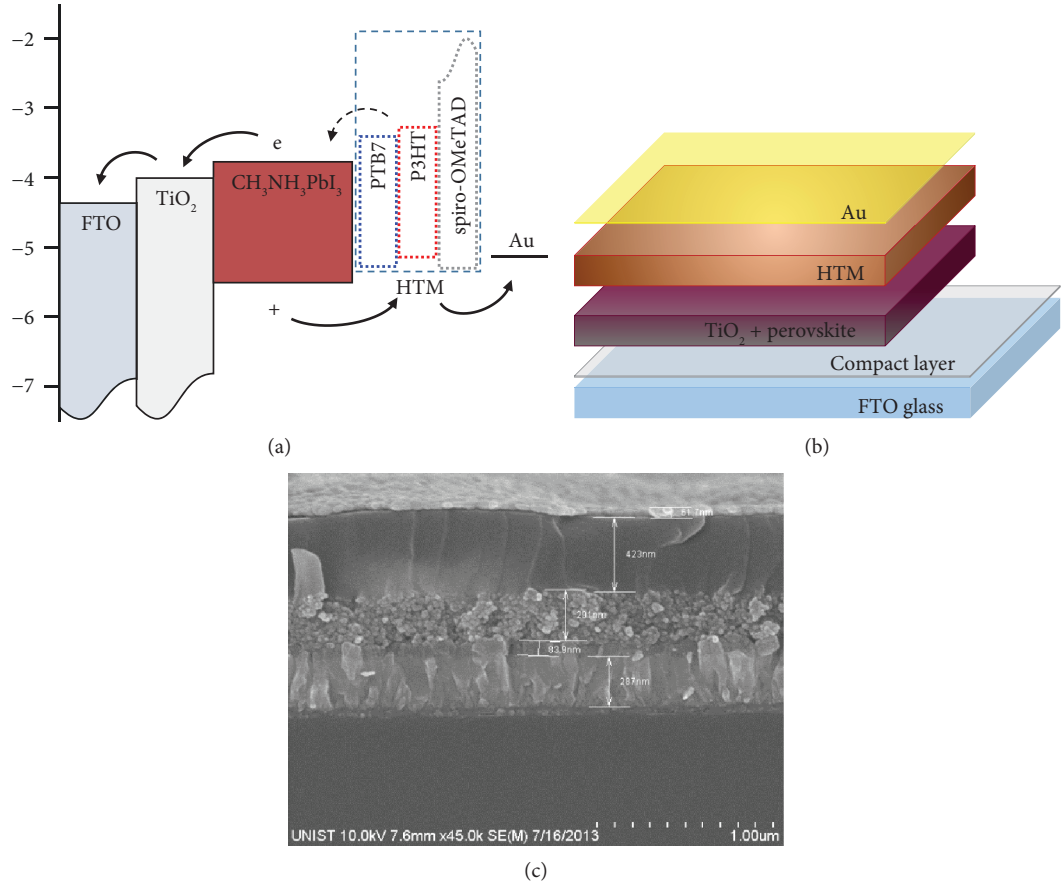

Figure 3: (a) Schematic of energy alignment of the different components. (b) Structure of the device architecture. (c) SEM image of the architecture.

UV spectra, the abovementioned criteria could be satisfied by the synthesized $CH_3NH_3PbI_3$ perovskite material.

Because of the high conductivity of perovskite materials, the thick layer of HTM should be coated onto the perovskite material in order to prevent the pinhole effect. However, a thick layer of HTM cause a high series resistance and decrease the efficiency of the device. Figure 2(a) shows the molecular orbital match of three different types of tested hole transport materials (spiro-OMeTAD, P3HT, and PTB7) with the other components of the device. Table 1 shows the HOMO and LUMO energy level as well as hole mobility value of three different HTM materials. The energy diagrams of each component are shown in Figure 2(b) with the HTM materials. From the previous report, spiro-OMeTAD was widely used as a hole conductor in $CH_3NH_3PbI_3$-based perovskite solar cells, and P3HT and PTB7 were generally used as an electron donor and/or hole transport material in organic solar cells. Notably, even though the P3HT and PTB are usually used as electron donor in organic electronic devices, here we used those materials as hole transport materials.

Figure 3(a) illustrates the energy levels of the system components and model of the charge separation processes; Figure 3(b) shows the schematic configuration of the device with the stacking of different components. In Figure 3(a), the tested HTM materials are energetically matched with perovskite sensitizer, and the energy level of the perovskite sensitizer is well positioned for the injection of electron into TiO_2 matrix and the injection of holes into the HTM Layer. A cross-sectional SEM image of the fabricated device is shown in Figure 3(c). In order to protect the electron recombination, a thin TiO_2 layer, called the "compact layer," was deposited onto the transparent conducting oxide (TCO). Mesoporous TiO_2 with metal-halide-based perovskite sensitizer as an active layer, HTM, and Au electrode was deposited in sequence. From the cross-sectional analysis, the thickness of spiro-OMeTAD, P3HT, and PTB7 layer was observed as 420 nm. The role of each HTM on the performance of the device is characterized separately. For that, solar cells containing different HTMs are used separately with the $CH_3NH_3PbI_3$-coated TiO_2 layer, and the individual device performance is measured under 1-sun illumination.

The photovoltaic parameters of all the three devices are extracted from the J-V curves (Figure 4) and are listed in Table 2. For comparison, without HTM (black, circle) sample was prepared. A metal-halide perovskite-sensitized cell without HTM shows a J_{sc} of 4.5 mAcm^{-2}, V_{oc} of 0.38 V, and FF of 44.7 with efficient (η) of 0.8%. The device made of spiro-OMeTAD- (red, circle) based HTM layer shows the best efficiency of 6.9% with a J_{sc} of 13.9 mAcm^{-2}, V_{oc} of 0.82 V, and

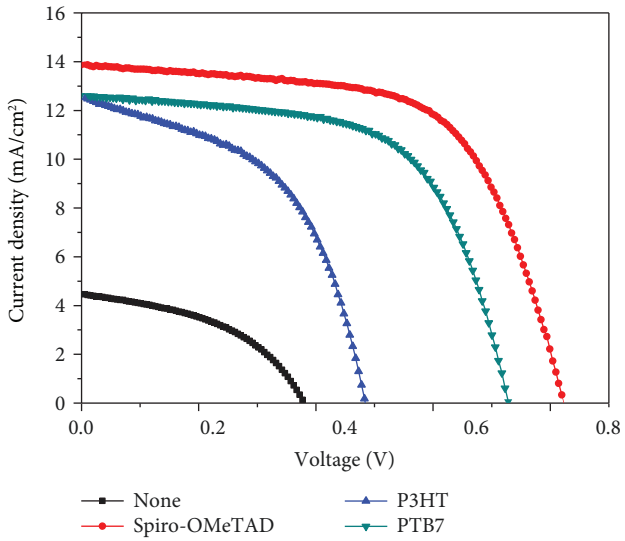

Figure 4: Photocurrent-voltage curves without HTM sample (black, circle), spiro-OMeTAD sample (red, circle), P3HT sample (blue, triangle), and PTB7 sample (cyan, triangle).

Table 2: Photovoltaic performance of the cells with various HTMs.

	J_{sc} (mA/cm^2)	V_{oc} (V)	FF (%)	Eff (%)
—	4.5	0.38	44.7	0.8
OMeTAD	13.9	0.82	60.2	6.9
P3HT	12.5	0.51	50.6	3.2
PTB7	12.6	0.72	60.4	5.5

FF of 60.2. Although P3HT is usually used as a hole conductor in organic solar cells, the device made with P3HT does not show a high efficiency in perovskite-based solar cells. In general, PTB7 is used as an electron donor for organic solar cells, but in perovskite solar cells, it plays a role of hole conductor at this study. The device made of PTB7 hole transport layer exhibits a J_{sc} of 12.6 mAcm^{-2}, V_{oc} of 0.72 V, FF of 60.4, and η of 5.5% by demonstrating a good charge-separation kinetics, and the efficiency value is comparable to the conventional spiro-OMeTAD-based device. Moreover, the thickness of the PTB7 hole transport layer is thinner (around 200 nm) than that of the spiro-OMeTAD layer (423 nm). In general, a thicker layer causes the higher series resistance of the device; however, the spiro-OMeTAD with a thinner layer of around 200 nm causes higher pinhole effects that may lead to the poor cell performance. In this work, we have demonstrated that PTB7 with a relatively thin hole transport layer showed the comparable efficiency value with the spiro-OMeTAD-based conventional cells. Obviously, P3HT and PTB7 show light absorption in UV range and also play a role of electron donor in organic solar cells; their role of hole transport behaviour in perovskite solar cell was confirmed using IPCE spectra.

Figure 5 shows the IPCE spectra of a device made of spiro-OMeTAD-based hole transport layer (black square) and PTB7 layer (red circle). The IPCE spectra of the cells

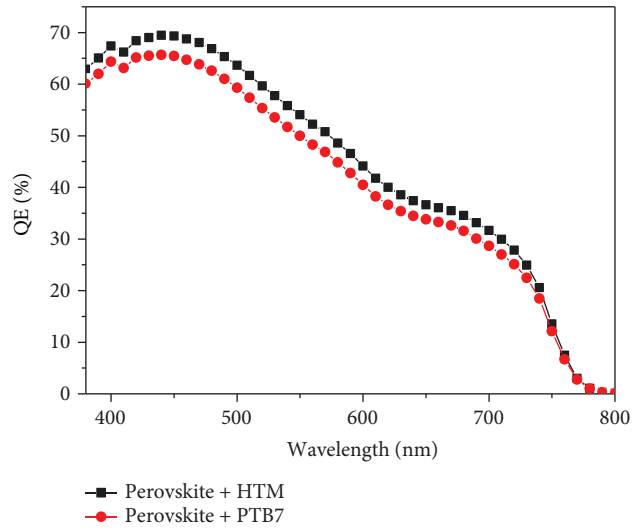

Figure 5: Incident photon to current conversion efficiency (IPCE) of the perovskite solar cells. Perovskite with spiro-OMeTAD (black, square) and perovskite with PTB7 (red, circle).

indicate that the devices show spectral responses from the near-infrared to visible regions, with the maximum photoresponse at ~450 nm and broader peaks extending to the infrared region. This IPCE spectra matched well with the UV-vis absorbance of the synthesized perovskite film as shown in Figure 1(b). However, polymer-based HTM cells do not show any other peculiar photoresponse for polymers, which confirms that here, the P3HT and PTB7 polymers play a role of only a hole conductor not as an electron donor.

4. Conclusions

In conclusion, we have demonstrated the solid-state solar cells with the $CH_3NH_3PbI_3$ organic perovskite material as the light absorber and three different organic hole transport materials. Among the three HTMs (spiro-OMeTAD, P3HT, and PTB7), spiro-OMeTAD cells show the best efficiency with 6.9% under AM 1.5 G. However, PTB7, which is a common electron donor material in organic solar cells, shows the hole transport behaviour in perovskite-based solid-state solar cells, and also a relatively thinner layer of PTB7 shows a good efficiency of 5.5%. Moreover, the energy level matching of these organic HTMs is well matched with the other components of the device. This interesting observation opens up the door for the investigation of different cost-effective materials for the highly efficient organic-inorganic hybrid solar cells in the near future.

Data Availability

The data used to support the findings of this study are available from the corresponding author upon request.

Conflicts of Interest

The authors declare that there are no conflicts of interest regarding the publication of this paper.

Acknowledgments

This research was supported by the KU Research Professor Program of Konkuk University.

References

[1] B. O'Regan and M. Grätzel, "A low-cost, high-efficiency solar cell based on dye-sensitized colloidal TiO_2 films," *Nature*, vol. 353, no. 6346, pp. 737–740, 1991.

[2] M. Grätzel, U. Bach, D. Lupo et al., "Solid-state dye-sensitized mesoporous TiO_2 solar cells with high photon-to-electron conversion efficiencies," *Nature*, vol. 395, no. 6702, pp. 583–585, 1998.

[3] M. Law, L. E. Greene, J. C. Johnson, R. Saykally, and P. Yang, "Nanowire dye-sensitized solar cells," *Nature Materials*, vol. 4, no. 6, pp. 455–459, 2005.

[4] J. Lim, M. Lee, S. K. Balasingam, J. Kim, D. Kim, and Y. Jun, "Fabrication of panchromatic dye-sensitized solar cells using pre-dye coated TiO2 nanoparticles by a simple dip coating technique," *RSC Advances*, vol. 3, no. 14, p. 4801, 2013.

[5] Y. Jo, J. Y. Cheon, J. Yu et al., "Highly interconnected ordered mesoporous carbon–carbon nanotube nanocomposites: Pt-free, highly efficient, and durable counter electrodes for dye-sensitized solar cells," *Chemical Communications*, vol. 48, no. 65, pp. 8057–8059, 2012.

[6] S. A. McDonald, G. Konstantatos, S. Zhang et al., "Solution-processed PbS quantum dot infrared photodetectors and photovoltaics," *Nature Materials*, vol. 4, no. 2, pp. 138–142, 2005.

[7] D. J. Milliron, S. M. Hughes, Y. Cui et al., "Colloidal nanocrystal heterostructures with linear and branched topology," *Nature*, vol. 430, no. 6996, pp. 190–195, 2004.

[8] A. J. Nozik, "Quantum dot solar cells," *Physica E: Low-dimensional Systems and Nanostructures*, vol. 14, no. 1-2, pp. 115–120, 2002.

[9] I. Robel, V. Subramanian, M. Kuno, and P. V. Kamat, "Quantum dot solar cells. Harvesting light energy with CdSe nanocrystals molecularly linked to mesoscopic TiO_2films," *Journal of the American Chemical Society*, vol. 128, no. 7, pp. 2385–2393, 2006.

[10] S. Günes, H. Neugebauer, and N. S. Sariciftci, "Conjugated polymer-based organic solar cells," *Chemical Reviews*, vol. 107, no. 4, pp. 1324–1338, 2007.

[11] W. U. Huynh, J. J. Dittmer, and A. P. Alivisatos, "Hybrid nanorod-polymer solar cells," *Science*, vol. 295, no. 5564, pp. 2425–2427, 2002.

[12] M. C. Scharber, D. Mühlbacher, M. Koppe et al., "Design rules for donors in bulk-heterojunction solar cells—towards 10 % energy-conversion efficiency," *Advanced Materials*, vol. 18, no. 6, pp. 789–794, 2006.

[13] B. C. Thompson and J. M. J. Fréchet, "Polymer–fullerene composite solar cells," *Angewandte Chemie-International Edition*, vol. 47, no. 1, pp. 58–77, 2008.

[14] H. J. Snaith, "Estimating the maximum attainable efficiency in dye-sensitized solar cells," *Advanced Functional Materials*, vol. 20, no. 1, pp. 13–19, 2010.

[15] A. Kojima, K. Teshima, Y. Shirai, and T. Miyasaka, "Organometal halide perovskites as visible-light sensitizers for photovoltaic cells," *Journal of the American Chemical Society*, vol. 131, no. 17, pp. 6050-6051, 2009.

[16] H. S. Kim, C. R. Lee, J. H. Im et al., "Lead iodide perovskite sensitized all-solid-state submicron thin film mesoscopic solar cell with efficiency exceeding 9%," *Scientific Reports*, vol. 2, no. 1, p. 591, 2012.

[17] M. M. Lee, J. Teuscher, T. Miyasaka, T. N. Murakami, and H. J. Snaith, "Efficient hybrid solar cells based on meso-superstructured organometal halide perovskites," *Science*, vol. 338, no. 6107, pp. 643–647, 2012.

[18] G. E. Eperon, V. M. Burlakov, P. Docampo, A. Goriely, and H. J. Snaith, "Morphological control for high performance, solution-processed planar heterojunction perovskite solar cells," *Advanced Functional Materials*, vol. 24, no. 1, pp. 151–157, 2014.

[19] M. J. Carnie, C. Charbonneau, M. L. Davies et al., "A one-step low temperature processing route for organolead halide perovskite solar cells," *Chemical Communications*, vol. 49, no. 72, pp. 7893–7895, 2013.

[20] J. H. Heo, S. H. Im, J. H. Noh et al., "Efficient inorganic–organic hybrid heterojunction solar cells containing perovskite compound and polymeric hole conductors," *Nature Photonics*, vol. 7, no. 6, pp. 486–491, 2013.

[21] J. Burschka, N. Pellet, S. J. Moon et al., "Sequential deposition as a route to high-performance perovskite-sensitized solar cells," *Nature*, vol. 499, no. 7458, pp. 316–319, 2013.

[22] D. Bi, S.-J. Moon, L. Haggman et al., "Using a two-step deposition technique to prepare perovskite ($CH_3NH_3PbI_3$) for thin film solar cells based on ZrO_2 and TiO_2 mesostructures," *RSC Advances*, vol. 3, no. 41, article 18762, 2013.

[23] D. Bi, L. Yang, G. Boschloo, A. Hagfeldt, and E. M. J. Johansson, "Effect of different hole transport materials on recombination in $CH_3NH_3PbI_3$ perovskite-sensitized mesoscopic solar cells," *The Journal of Physical Chemistry Letters*, vol. 4, no. 9, pp. 1532–1536, 2013.

[24] E. Edri, S. Kirmayer, D. Cahen, and G. Hodes, "High open-circuit voltage solar cells based on organic–inorganic lead bromide perovskite," *The Journal of Physical Chemistry Letters*, vol. 4, no. 6, pp. 897–902, 2013.